



Cite this: *Green Chem.*, 2026, **28**, 1787

Accelerated biodegradation of polyurethanes through embedded cutinases

Daniela Knopp,^a Simone Göbbels, ^a René Münchrath,^a Cristina Lavilla Aguilar,^b Michael Kessler,^a Qi Chen, ^b Marian Bienstein, ^c Linda Katharina Wiedemann,^a Jonas Gerund,^a Edward Zoet,^b Gernot Jäger,^a Ulrich Schwaneberg ^{*c} and Lukas Reisky ^{*a}

Polyurethanes (PUs) are a versatile class of synthetic polymers, which are widely used in foams, coatings, and adhesives. The chemical composition of PUs makes them resistant to biodegradation and causes challenges in applications in which recycling is not an economically viable option, such as plant fixing clips, or tree shelters. A sustainable use in the latter applications requires PU-polymers designed for effective biodegradation with minimized ecological footprints. In this study, a proof of concept for accelerated degradation of biodegradable biocomposite PU materials has been achieved. The PU material was made from thermoplastic PUs (TPUs) and four thermostable cutinases, that were incorporated into industrially important TPUs via melt extrusion at standard TPU processing temperatures up to 200 °C. Embedded cutinases yielded a 37% enzymatic hydrolytic degradation in *in vitro* studies and biodegradation was accelerated up to ninefold at close to application conditions in activated sludge when compared to virgin TPU. Cutinase-accelerated TPU degradation is a step forward towards a responsible end-of-life waste management within a circular PU economy.

Received 9th July 2025,
Accepted 29th September 2025

DOI: 10.1039/d5gc03512k
rsc.li/greenchem

Green foundation

1. Our research advances the field of green chemistry by developing biodegradable thermoplastic polyurethanes (TPUs) through the incorporation of thermostable cutinases *via* melt extrusion at industrial relevant TPU processing temperatures.
2. Our key achievement was to demonstrate that TPU containing embedded HiC showed 31.1% biodegradation in activated sludge which is nearly ninefold higher than the original TPU. The cutinases retained activity after being incorporated at temperatures up to 200 °C, enabling compatibility with standard industrial manufacturing.
3. Future work should include a full characterisation of biodegradation pathways, a validation of the performance through field testing in diverse environments, and comprehensive life cycle assessments.

Introduction

Polyurethanes (PUs) are versatile polymers with unique properties in respect to durability, flexibility, and resistance to abrasion and chemicals, all of which can be tailored to meet specific requirements in numerous applications.^{1,2} Development of PUs dates back to the late 1930s and the first commercial production started in the 1940s.³ PU syntheses involve the reaction of isocyanates (aliphatic or aromatic) with polyols, for which polyether (PE), or polyester (PES) types are

typically used.¹ In a thermoplastic PU (TPU) for example, the urethane-containing crystalline regions referred to as hard segments, contribute to stiffness and recalcitrance.^{2,4–6} The PES-containing amorphous regions, referred to as soft segments, contribute to TPU-flexibility.^{2,5,7,8} Composition of monomeric building blocks determines mechanical and physical properties of PUs and can be tailored to match application demands such as foams, coatings, adhesives and sealants, elastomers, and textiles.¹

As PUs are broadly used, a steady growth in global production has occurred reaching a global market valued at 73 billion USD in 2024 with a projected growth forecast to 102 billion USD until 2033, ranking PUs in 6th place for commonly produced plastics.^{9,10} High PU demand generates substantial solid waste estimated at approximately 2.1 to 3.6 million tons per year in Europe alone, solely from PU foams.¹¹ From these

^aCovestro Deutschland AG, Kaiser-Wilhelm-Allee 60, 51373 Leverkusen, Germany.
E-mail: lukas.reisky@covestro.com

^bCovestro Netherlands B.V., Urmonderbaan 22, 6167 RD Geleen, Netherlands

^cInstitute of Biotechnology, RWTH Aachen University, Worringerweg 3, 52074 Aachen, Germany. E-mail: u.schwaneberg@biotec.rwth-aachen.de



amounts about 43%–50% of PU waste ends up in landfill^{12,13} and about 33% is incinerated for energy production, contributing to global warming through CO₂ emissions.¹² Landfill and incineration account for >70%, which impressively illustrates the need for a circular PU economy. Notably, PUs cause environmental challenges in soil^{13–15} and marine ecosystems.^{16–18} In sectors, such as agriculture, plastic products remain within the environment, without economic recycling possibilities. Examples include seed coatings, plant fixing clips, or tree shelters.¹⁹ Biodegradation is an important desired feature of PUs, especially when sustainable reuse is not feasible.

Over the past decades, numerous studies have examined PU degradability and the impact of PU presence in the microbiome of various environmental habitats.²⁰ Investigated conditions range from challenging environments with low microbial density and low temperatures, such as seawater,²¹ to biologically active soils at 25 °C (moderate composting),²² and industrial composting conditions at 58 °C.^{22–24} These studies report that the speed and efficiency of biodegradation are strongly influenced by the habitat, with higher rates observed in microbial-rich soil.^{22–25} Still, PU breakdown took weeks to years with some of the studies reporting mineralization rates below 30% after 50 days²⁵ which neither meets the criteria for biodegradability nor for industrial composting (European Commission; DIN EN 13432).²⁶ The reported results confirm the high resistance of PU to biodegradation and its often-intended long-term use in applications. Biodegradation efficiency depends on the polymer's chemistry with PES-based PU being more prone to microbial attack due to its ester groups in the soft segments, whereas PE-based PU resists biodegradation, but rather decomposes through oxidation.^{14,27–30} Many different bacterial and fungal species are involved in the biodegradation of PUs.^{27,31–33} The biodegradation of PES-PU is initiated by the cleavage of ester bonds, which serves as a rate-limiting step in the hydrolytic degradation process.³⁴ Ester-bond hydrolysis can efficiently be catalysed by enzymes, which makes hydrolases, such as lipases and cutinases, the primary enzyme class for PES-PU biodegradation.^{34–37}

Cutinases (EC 3.1.1.74) are reported to efficiently degrade polyethylene terephthalate (PET).^{38–43} Cutinases are extracellular enzymes that belong to the serine hydrolase family within the α/β -hydrolase superfamily, characterized by a Ser-His-Asp catalytic triad.⁴⁴ Their ability to degrade polyesters makes them of high interest for current plastic degradation processes.⁴⁴ A common feature of all cutinases is the absence of a lid structure, which covers the active site of other hydrolases such as lipases. The exposed active site in cutinases facilitates binding to insoluble substrates such as PET and PU.⁴⁴ One study showed high degradation rates of the PES-based PU dispersion Impranil® DLN-SD by the cutinases TfCut2 and Tcur0390.³⁵ Another study reported improved substrate specificity of TCur1278 by combining the cutinase with a polymer-material binding peptide, which significantly accelerated the degradation of Impranil® DLN-SD under ambient conditions.⁴⁵ Solid PES-PU degradation has been verified with the fungal cutinase BaCut1 from *Blastobotrys* sp. G-9 and with HiC

from the thermophilic fungus *Humicola insolens*, by hydrolysis of intramolecular ester bonds.^{46,47} Noteworthy a high number of cutinases are thermostable with melting temperatures (T_m) ≥ 80 °C. Examples are the cutinase 1 and its variants from *Thermobifida cellulosilytica*,⁴⁸ the engineered Cut190*,⁴⁹ as well as variants from the LCC,⁵⁰ and HiC.⁵¹ Cutinases have promising properties to develop biodegradable plastics, especially if embedded into PU which is intended for environmental applications. Previous research demonstrated an improved degradability of poly lactic acid (PLA) by an extrusion-based incorporation of proteinase K immobilized with polyacrylamide. The degradation study verified enzyme activity after incorporation at 200 °C.⁵² In another study an engineered PLAase was incorporated into PLA *via* film extrusion at 160 °C. 70% PLA-film degradation after an incubation at 45 °C for 3 days in an aqueous system was reported.⁵³ Further reported examples employed for instance HiC for polyester hydrolysis of polycaprolactone (PCL), poly(butylene succinate-*co*-adipate) (PBSA), poly(butylene succinate) (PBS), poly(butylene adipate-*co*-terephthalate) (PBAT), poly(*D*-lactic acid) (PDLA), and poly(ethylene 2,5-furanoate) (PEF). Melt extrusions were successfully performed at temperatures between 90 °C and 205 °C.⁵⁴ HiC was actively incorporated at processing temperature up to 175 °C for PDLA (22% degradation),⁵⁴ while at 205 °C no HiC activity could be detected.⁵⁴ The mentioned reports predominantly focus on polymers that are already classified as biodegradable plastics under certain conditions (except PEF).⁵⁵ As a general trend one has to acknowledge that classical biodegradable polymers do often not match performance properties required in applications and can therefore not replace all PU products, where biodegradable alternatives are essential. For instance, unmatched are tensile strength, abrasion resistance and hardness as well as flexibility at the same time of PUs. PU, besides PET, is one of the two most abundant plastic types featuring a hydrolysable backbone, particularly in the case of PES-PU.^{1,56} An increased ratio of hard to soft segments enhances mechanical properties such as compressive strength and resistance to mechanical abrasion, which is required for instance in caster wheels.^{1,2} Hard segments increase crystallinity and T_m , which makes the incorporation of bioactive compounds *via* melt extrusion challenging.^{57,58} One study reported incorporation of microbial spores into a low melting TPU at 135 °C, which resulted in twice as fast TPU degradation after 5 months of incubation.⁵⁹ The employed processing temperature of 135 °C for spore embedment is however lower than the typical processing temperature range for TPUs, which are generally between 145–210 °C,^{60–63} allowing for formulation- and process-specific variations. No process has been described so far for the incorporation of enzymes or spores into TPU at standard processing temperatures, which is often necessary to achieve a homogeneous distribution during additive compounding.⁶³

The aim of this study was to show a proof of concept to embed cutinases at standard TPU-processing temperatures to enable development of biodegradable TPUs with the long-term aim to reduce plastic pollution in nature. Proof of concept has been achieved by investigating four thermostable cutinases



(HiC: Novozym® 51032,⁵¹ ThcCut1-ACCG, SvCut190*SS and LCC-ICCG), which were embedded into TPU *via* melt extrusion at processing temperatures up to 200 °C. Degradation studies under laboratory conditions were performed and confirmed HiC-catalysed TPU degradation after processing temperatures up to 200 °C. Up to a processing temperature of at least 160 °C an accelerated TPU degradation of embedded compared to externally supplemented HiC could be achieved, which proves that embedment enhances TPU degradation kinetics. Additionally, studies of TPU embedded with all four cutinases in activated sludge were performed according to the OECD 301 F protocol^{26,64} and again HiC accelerated the TPU biodegradation in activated sludge.

Experimental section

A detailed description of the experimental procedures is provided in the SI.

Materials

All reagents were purchased from commercial sources. TPU samples were sourced from Covestro Deutschland AG (Leverkusen, Germany). The two *Escherichia coli* (*E. coli*) strains DH5α and BL21(DE3) were acquired from Fisher Scientific (Schwerte, Germany). The cutinase Novozym® 51032, reported as cutinase from *Humicola insolens* (HiC),⁵¹ was obtained from Strem Chemicals (Bischheim, France).

Methods

Preparation of HiC lyophilisate. For incorporation and heat tests, buffer exchange (20 mM ammonium acetate buffer, pH 8.0) was conducted with the purchased HiC stock solution using crossflow filtration (Vivaflow® 50 cassette; Sartorius, Göttingen, Germany). The HiC solution was frozen at -80 °C, freeze-dried (-68 °C, 0.1 mbar, 3 days; alpha 1-2 LDplus, Martin Christ Gefriertrocknungsanlagen GmbH, Osterode am Harz, Germany), and the obtained powder was stored at 4 °C until further use.

Cutinase expression and purification. Genes for BhrPETase, DuraPETase^{N233K}, and SvCut190*SS were synthesized by Eurofins Genomics (Ebersberg, Germany) and cloned into the pET26b(+) vector using restriction cloning. The same method was used for LCC, LCC-ICCG, LCC-WCCG, and ThcCut1. PES-H1 gene was cloned into PET28a(+), and TfCut2 gene into the pBAD expression vector. ThcCut1-ACCG⁴⁸ was derived from the wild-type ThcCut1 gene *via* mutation polymerase chain reaction (Biometra TAdvanced 96 SG, 230 V, Göttingen, Germany) and cloned into the pET26b(+) vector. *E. coli* DH5α cells were transformed for plasmid amplification, and cultures were preserved with 20% (v/v) glycerol and stored at -80 °C. For sequencing at GeneWiz (Leipzig, Germany) plasmid isolation was performed using the GeneJET Plasmid Miniprep kit from Thermo Fisher Scientific (Darmstadt, Germany) according to the manufacturer's protocols.

For cutinase expression *E. coli* strain BL21(DE3) was transformed with the respective plasmid constructs. Pre-cultures were prepared in Lysogeny broth (LB) medium supplemented with 1% glucose and 50 µg ml⁻¹ kanamycin (Kan50) or 100 µg ml⁻¹ ampicillin (Amp100). Cultures were incubated overnight at 37 °C (ISF1-X, Adolf Kühner AG, Birsfelden, Switzerland). Cutinase expression was done using the autoinduction medium ZYP-5052,⁶⁵ supplemented with the appropriate antibiotic (Kan50 or Amp100) (Table S1). *E. coli* cultures containing the pBAD expression system were cultivated in LB medium and cutinase expression was induced with 0.2% (v/v) L-arabinose. Both main cultures were inoculated with 0.2% (v/v) of the overnight pre-cultures. Expression cultures were cultivated for 4.5 h at 37 °C, followed by 24 h at 20 °C (ISF1-X). Cells were harvested by centrifugation (8000g, 4 °C, 20 min; Multifuge X4R Pro, Thermo Fisher Scientific, Waltham, USA).

Harvested cells were resuspended in either KPi buffer (20 mM, pH 7.5; not intended for enzyme purification) or in imidazole-containing lysis buffer (50 mM NaH₂PO₄, 300 mM NaCl, and 10 mM imidazole, pH 8.0; intended for purification *via* affinity chromatography). Cell lysis involved three two-minute sonication cycles (Bandelin Sonoplus HD, Sonotrode MS73, Berlin, Germany), at 50% amplitude with constant sample cooling. Lysates were centrifuged (10 000g, 4 °C, 20 min; Multifuge X4R Pro) and filtered (0.2 µm sterile PES filter) to obtain the cleared soluble enzyme fraction which was then frozen at -80 °C and subsequently freeze-dried (-68 °C, 0.1 mbar, 3 days; Alpha 1-2 LDplus). Lyophilised cutinase powders were stored at 4 °C until further use.

Cutinase purification *via* immobilized metal affinity chromatography (IMAC) was performed with the SvCut190*SS which was expressed both without and with a His-tag. Ni-NTA (HisPur™ Ni-NTA Resin) purification columns were equilibrated with imidazole-containing lysis buffer. Filtered lysate containing the soluble fraction of SvCut190*SS was applied to the column, followed by column washing with wash buffer (50 mM NaH₂PO₄, 300 mM NaCl, 20 mM imidazole) and elution with elution buffer (50 mM NaH₂PO₄, 300 mM NaCl, and 250 mM imidazole, pH 8). Elution fractions were pooled and concentrated with Amicon® Ultra centrifugal filters (10 kDa MWCO). Desalting of the concentrated SvCut190*SS solution was performed using PD-10 columns according to the manufacturer's instructions. Buffer exchange was done with KPi (20 mM, pH 7.5). The cutinase solution was freeze-dried as previously described (-68 °C, 0.1 mbar, 3 days; Alpha 1-2 LDplus) and the obtained powder was stored at 4 °C until further use.

Determination of protein concentration and quantification of cutinase activity. Protein concentration was quantified with the Bradford assay and a bovine serum albumin (BSA) standard curve (125 to 1000 µg ml⁻¹). Dry cutinase lyophilisate was dissolved in water at room temperature, filtered (0.2 µm sterile PES filter), and diluted if necessary. For the assay, 5 µl of BSA or cutinase sample and 250 µl of Quick Start Bradford Reagent 1× (Pierce™ Bradford Plus Protein Assay Reagent, Thermo Scientific, Rockford, USA) were mixed. The samples were incu-



bated for 5 minutes at 30 °C, and absorbance was measured at 595 nm with a microplate reader (Varioskan LUX, Thermo Fisher Scientific, Waltham, USA). All measurements were performed in triplicates or duplicates.

Hydrolytic activity of cutinases was measured by monitoring *p*-nitrophenol (*p*NP) release from *p*-nitrophenyl butyrate (*p*NPB) hydrolysis at the maximum absorbance peak of *p*NP at 410 nm. A *p*NP standard curve (0.001–0.05 mg ml⁻¹) was measured (Varioskan LUX) to determine the extinction coefficient. Sample preparation was performed as described for the Bradford assay, but dissolving and dilutions were done with KPi buffer (100 mM, pH 7.5). For the assay, 20 µl of cutinase solution and 180 µl *p*NPB substrate solution (0.5 mg ml⁻¹ diluted in 100 mM KPi buffer, pH 7.5) were mixed in a 96 well microplate. *p*NP increase was measured kinetically at 30 °C every 15 seconds for 15 minutes (Varioskan LUX). Measurements were performed in triplicates or duplicates. The volumetric activity was calculated with the following equation:

$$\text{Volumetric activity [U ml}^{-1}\text{]} = \frac{\Delta\text{OD}_{410\text{ nm}} \times V_M \times V_F}{d \times V_e \times \epsilon}$$

where: $\Delta\text{OD}_{410\text{ nm}}$ = kinetic slope in linear range at 410 nm [absorbance/min], V_M = reaction volume [ml], V_F = dilution factor, d = thickness of microplate wall [cm], ϵ = molar extinction coefficient of *p*NP [l (mol cm)⁻¹], V_e = sample volume [ml]

Specific activity was calculated based on protein concentration (mg). One cutinase unit (U) is defined as the amount of cutinase (mg) releasing one µmol of *p*NP per minute under the tested conditions.

Heat tolerance tests with simultaneously incorporation into polyester polyol. Cutinases were tested for thermotolerance between 100 °C and 200 °C using a low melting polyester polyol made from adipic acid, ethylene glycol and butane diol. Molten polyester polyol was mixed with 0.5 wt% cutinase lyophilisate and incubated at 100 °C for 60 minutes with 1500 rpm agitation in a heating block (ThermoMixer® C, Eppendorf SE, Hamburg Germany). Samples were taken by transferring the molten polymer to a metal flat washer and allowing it to cool down and harden at room temperature.

For temperatures above 100 °C molten polyester polyol was weighed into a round bottom flask and again mixed with 0.1 wt% cutinase lyophilisate. The mixture was heated using an oil bath (Korasilon M100) placed on a magnetic stirrer (IKA® RCT basic S000, IKA-Werke, Staufen im Breisgau, Germany) to ensure well mixing. Heating temperature was gradually increased to 200 °C and polymer samples were taken every 10 °C increase in temperature and transferred to a metal flat washer for cooling.

Phenol red assay. Platelets from cutinase lyophilisate incubation and incorporation in polyester polyol at 100 °C were applied in a qualitatively cutinase activity study with the pH indicator phenol red. Samples (50–60 mg) were weighed into tubes and 1000 µl of KPi buffer (100 mM, pH 7.5, Kan50 and Amp100) was added. For positive controls (external addition of cutinase: 0.9–1.8 wt%) 900 µl of KPi buffer was added. Subsequently, 50 µl of the phenol red stock solution (1 mg

ml⁻¹ phenol red in 20% v/v ethanol) was added to each tube. Samples were incubated for 3 h at 30 °C and for 15 h at 40 °C with 900 rpm agitation in a heating block (ThermoMixer® C). Acid release, indicated by a yellow colour change, was documented photographically.

Quantification of cutinase activity with pH-stat system. Ester hydrolysis activity of cutinases incubated at temperatures above 100 °C in molten polyester polyol was assessed by a pH-stat pre-screening assay using the BioLector® Pro micro-fermentation system (Beckman Coulter Life Sciences, Brea California, United States), in combination with the microfluidic microplates (FlowerPlate®, Beckman Coulter Life Sciences). With this assay sodium hydroxide (NaOH, 3 M) consumption was measured during ester bond hydrolysis in polymer samples incubated in aqueous buffer (KPi, 100 mM, pH 7.0, Kan50). The measurement principle relies on NaOH titration to maintain a constant reaction pH upon acid release during enzymatic ester hydrolysis from the investigated polymer samples. Titration was automated and controlled by the BioLector® Pro system. The total amount of consumed NaOH over the reaction time serves as a measure for enzymatic degradation activity. For the screening assay, polymer samples (approximately 50 mg), with or without incorporated cutinase, were weighed into each culture well of the microplate, ensuring equal particle size. KPi was added to all samples. In the positive controls, 0.1 wt% dissolved cutinase lyophilisate was added externally. Samples without any cutinase additions were used as negative controls to determine auto hydrolysis. All reactions were single measurements, incubated for up to 94 h (HiC only 45 h) at 30 °C, pH set at 7.0, and 600 rpm under 85% humidity in the BioLector® Pro, monitoring the base consumption over time.

Gel permeation chromatography (GPC). Number-average molecular weight (M_n) and dispersity index of TPUs were measured by GPC using an Agilent 1260 Infinity II system equipped with a refractive index detector (Agilent 1260 MDS) and two PLgel Mixed C columns (300 × 8 mm; Agilent, Santa Clara, USA). Each TPU sample was dissolved in dimethylformamide (DMF, supplemented with 0.01 M sodium nitrate) at a concentration of 5 mg ml⁻¹. Samples were heated at 60 °C for 1 hour, homogenized well and filtered (0.45 µm PTFE filter) prior to GPC analysis. 100 µl of each dissolved TPU sample was injected into the GPC system and separated by size using DMF with 0.1 M sodium nitrate as mobile phase with a flow rate of 1 ml min⁻¹. Data analysis was performed using Agilent GPC/SEC software. M_n was calculated by comparing the elution time of narrow polystyrene standards of known molar mass with the elution profile of the TPU.

Enzymatic degradation studies of TPUs under laboratory conditions. TPU samples (Table 1) were dried (70 °C, 24 h; FD 115, Binder GmbH, Tuttlingen, Germany) previously to degradation studies. 200 mg of each TPU was placed in a 15 ml tube. KPi buffer (200 mM, pH 8.0, Kan50, Amp100, and 300 µg ml⁻¹ hygromycin B: Hyg300) and 5% (v/v) of sterile filtered HiC were added to a final volume of 10 ml. For the extrusion pre-tests, TPU 4 and 5 were used with varying cutinase concen-



Table 1 Composition of thermoplastic polyurethanes evaluated in this work

TPU name	Number-average molecular weight (M_n) (g mol $^{-1}$)	Dispersity index	Polyester polyol content	Composition of soft segment	Composition of hard segment
TPU 1	125 000	1.53	35 wt%	Poly(1,4-butylen adipate)	1,4-butanediol Methylene diphenyl diisocyanate
TPU 2	87 800	1.42	50 wt%	Poly(1,4-butylen adipate)	1,4-butanediol Methylene diphenyl diisocyanate
TPU 3	115 000	1.42	55 wt%	Poly(1,4-butylen adipate)	1,4-butanediol Methylene diphenyl diisocyanate
TPU 4	101 000	1.46	70 wt%	Poly(1,4-butylen adipate)	1,4-butanediol Methylene diphenyl diisocyanate
TPU 5	87 100	1.71	60 wt%	Poly(1,4-butylen adipate) Lactide	1,4-butanediol Hexamethylene diisocyanate

trations (0.1, 0.3, 0.5, 0.8 and 1 wt% relative to the polymer) in a total KPi reaction volume of 5 ml. Cutinase lyophilisate of HiC, ThcCut1, TheCut1-ACCG, SvCut190*SS, LCC-ICCG, and pET26b_EV was dissolved in demineralised water and sterile filtered to prepare stock solutions. All TPU samples were incubated in a heating block (ThermoMixer® C) at 37 °C and 200 rpm for 32–33 days. Adipic acid was quantified *via* high performance liquid chromatography (HPLC) analysis (Agilent 1260 Infinity II system, Santa Clara, USA). Weight loss was measured after washing the samples two times with demineralised water and drying them at 70 °C for 24 h. Samples were weighed with a microbalance (Cubis®-1442AC MSA225S-110-DI, Sartorius, Göttingen, Germany).

Preparation of cutinase-embedded TPUs *via* melt extrusion.

TPU samples were dried (70 °C, 48 h; FD 115) and in the case of TPU 4 milled to a particle size of ≤ 1 mm under liquid nitrogen flow (MM 500 Nano, Retsch GmbH, Haan, Germany). For the incorporation of cutinases into TPUs, a twin-screw microcompounder (Xplore MC 15, Xplore Instruments BV, Sittard, Netherlands), was used. Cutinases were prepared as non-purified cell free lyophilised extracts from cutinase expression (crude lyophilised clarified lysate) or additionally as purified extract (SvCut190*SS). For HiC, the commercial purchased stock was used as desalted lyophilised powder. Premixes of TPU and cutinase powder were prepared as listed in Table S2, to ensure a homogenous distribution during the extrusion process. HiC, was incorporated in three ways: (i) 0.3 wt% HiC, (ii) 0.3 wt% NHS-labelled HiC (at 150 °C), and (iii) 0.033 wt%, where the last concentration was to compare with the lowest cutinase activity of LCC-ICCG (0.023 pNPB U per mg TPU).

The compounder was flushed with TPU followed by one premix of TPU/cutinase before each new sample batch to avoid contamination between batches. Compounding was performed for a total of 1.5 minutes (≤ 1 minute filling time) at the set temperature (Table S2), with a rotation speed of 50 rpm. Samples were cooled down at room temperature and dried (70 °C, 24 h; FD 115) before degradation studies.

For mechanical characterisations tension rods were prepared with HiC and TheCut1-ACCG with a concentration of 0.3 wt% relative to the TPU weight. TPU 4 was processed at 210 °C and TPU 5 at 180 °C, then injected into a micro-injection moulding machine (Xplore 12cc, Xplore Instruments BV, Sittard, Netherlands), to form the dumb bell test specimen shape of type 5A.

Enzymatic degradation studies of extruded TPU granules with embedded cutinases under laboratory conditions. Degradation studies of cutinase-embedded TPU samples were conducted in deep-well plates with 200 mg of each previously dried (70 °C, 24 h; FD 115) TPU. Samples were weighed in triplicates. 5 ml of KPi buffer (200 mM, pH 8.0, Kan50, Amp100, Hyg300) was added to samples with embedded cutinases and negative controls without cutinase addition. To TPU samples intended for positive controls the same KPi buffer was added to a final volume of 5 ml, as well as 0.3 wt% dissolved cutinase (relative to the TPU weight). Cutinase stocks were prepared by dissolving cutinase lyophilisate in demineralised water fol-

lowed by sterile filtration. Deep-well plates were sealed with an aluminium self-adhesive foil and incubated at 37 °C, 150 rpm for 21 days. Samples were taken for adipic acid quantification *via* HPLC analysis. After the total incubation period, solid samples were washed two times with demineralised water, dried (70 °C, 24 h; FD 115) and stored at room temperature for further analyses.

HPLC measurements. Samples for HPLC analysis were filtered (0.2 µm PVDF filter), and the pH was adjusted with 1% (v/v) phosphoric acid. An Agilent 1260 Infinity II system equipped with a multisampler (G7167A), a diode array detector for UV and visible light range, and a Zorbax Eclipse Plus C18 column (4.6 mm × 150 mm, 5 µm, Agilent, Santa Clara, USA), was used. Adipic acid was quantified with a gradient method, with an aqueous mobile phase (0.085% v/v phosphoric acid in demineralised water) and 99.8% acetonitrile (Table S3) at a column temperature of 35 °C. The flow rate was 1.5 ml min⁻¹, and 5 µl of the sample was injected. Data analysis was performed using the Chromeleon Chromatography Data System 7.3.1 software (Thermo Fisher Scientific, Waltham, USA).

Light and scanning electron microscopy (SEM). Washed and dried TPU samples were investigated *via* light microscopy (DM2700 M microscope; Leica Microsystems, Wetzlar, Germany) and SEM (TM4000 Plus tabletop device; Hitachi, Tokyo, Japan) after degradation studies. Whole TPU samples and cut surfaces were analysed. The SEM pictures were taken at 15 kV acceleration voltage under medium vacuum using secondary or backscatter electrons.

HiC staining and fluorescent microscopy. HiC was labelled with NHS-fluorescein (5/6-carboxyfluorescein succinimidyl ester) according to Huang *et al.* (2023).⁵⁴ Briefly, 80.66 mg HiC lyophilisate was dissolved in 14.4 ml demineralised water and 13.87 mg NHS-fluorescein was dissolved in 1.6 ml dimethyl sulfoxide. The solutions were combined and incubated for 4 h at room temperature in the dark. Excess dye was removed *via* buffer exchange (20 mM KPi, pH 7.5) with a PD-10 column. The solution was frozen at -80 °C and subsequently freeze-dried as previously described (-68 °C, 0.1 mbar, 3 days; Alpha 1-2 LDplus). The lyophilisate was incorporated into TPU 5 *via* melt extrusion at 150 °C.

For fluorescent microscopy, 20 µm thick microtome cuts were produced with a rotary microtome (HM 355 S, Microm International GmbH, Dreieich, Germany). Samples were inspected using a Leica DM6000 microscope (Leica Microsystems, Wetzlar, Germany) with fluorescence mode (band-pass filter of 420–490 nm for excitation; long pass filter of 515 nm for emission).

Atomic force microscopy (AFM) and infrared photo-induced force microscopy (PiFM). TPU samples were prepared for AFM and PiFM by cryo-cutting (knife temperature: -30 °C; specimen and cryochamber temperature: -130 °C; cutting speed: 1 mm s⁻¹) of even block faces in transverse direction using a Leica EM UC7/FC7 ultramicrotome (Leica Microsystems, Wetzlar, Germany) with diamond knives (knife angle 45°, clearance angle 6°).

TPU microtome cuts were placed on an AFM sample stub and imaged under ambient conditions in tapping mode using

a Dimension Icon multimode AF microscope (Bruker Nano Surfaces, Madison, United States) with silicon cantilevers and resonance frequencies of 300–400 kHz (model: TESP, Bruker Nano surfaces).

PiFM was performed with a Vista 75 microscope (Molecular Vista, Inc., San Jose, United States) and a laser wavelength of 800 to 1800 cm⁻¹ (spectral line width 1 cm⁻¹) using the MIRcatTM mid-infrared (IR) quantum cascade laser (QCL). A platinum-iridium coated AFM cantilever (NCH-300 kHz, Nanosensors Inc., Neuchatel, Switzerland) was used oscillating at the second mechanical resonance frequency (f_2), to measure surface topography and at the first mechanical resonance frequency (f_1) to detect photo-induced force. The laser was modulated at the difference frequency ($f_1 - f_0$) with an average power of 1 mW. Images were recorded at 256 × 256 pixels (scan rate: 0.5 Hz; setpoint: 75%; amplitude: 2 nm). PiF spectra were acquired using an acquisition time of 26 s per spectrum over the set spectral range. The spectra were laser power normalized and smoothed. An IR spectrum of HiC lyophilisate was measured for data evaluation using a Tensor II spectrometer (Bruker Nano surfaces) equipped with an attenuated total reflection unit. The spectrum, recorded in absorbance mode between 400–4000 cm⁻¹, was obtained by a total of 16 scans.

Mechanical studies. Tensile tests with TPUs before degradation studies were performed using a Zwick testing machine (ZwickRoell GmbH & Co. KG, Ulm, Germany) according to ISO 527-01. Measurements were conducted with a tensile speed of 200 mm min⁻¹ with at least two dumbbell test specimen type 5A (75 mm × 4 mm × 2 mm) at room temperature.

Solution viscosity determination. Solution viscosity of TPU samples before degradation studies was determined using a Stabinger viscometer (SVM3000/G2, Anton Paar, Graz, Austria) with sample solutions of 0.4 wt% TPU, dissolved in *N*-methyl pyrrolidone (NMP) at approximately 70 °C. After solutions equilibrated overnight the kinematic viscosity (ν) was measured at 25 °C. Pure NMP was used as blank at the beginning and end of each measurement series. The relative viscosity was calculated according to the following equation:

$$\text{Relative viscosity [mm}^2 \text{s}^{-1}\text{]} = \frac{\phi\nu \text{ of sample solutions}}{\phi\nu \text{ of blanks}}$$

Differential scanning calorimetry (DSC) analysis. DSC measurements were performed with 10 mg TPU sample using a Netzsch Polyma 214 DSC device (NETZSCH-Gerätebau GmbH, Selb, Germany). Three cycles were conducted: heating from -75 °C to 260 °C, cooling to -75 °C, and reheating to 260 °C at 20 K min⁻¹. The DSC analysis determined the glass transition (T_g) and the melting temperature (T_m), as well as the crystallisation and melting enthalpies.

Biodegradation studies of extruded TPU granules with embedded cutinases. Biodegradation tests with activated sludge followed the OECD (Organisation for Economic Co-operation and Development) 301 F manometric respirometry method, using the BD600 system (Tintometer GmbH, Lovibond Water Testing, Dortmund, Germany).



Briefly, required amounts of polymer test substance/sodium acetate control/cellulose control were calculated based on the theoretical oxygen demand (ThOD). The test medium included activated sludge, demineralised water, and salt as well as trace element solutions A–D specified in OECD 301 A, section 5 (phosphate buffer, CaCl_2 , MgSO_4 , and FeCl_3). All solutions were aerated at 20 °C for 20 minutes. Biodegradability studies were conducted in duplicates, with sodium acetate as a positive control ensuring proper equipment function and microbial activity, and a blank sample without test substance. The test substance was added to glass bottles, with 157 ml of test medium and 5 drops of allylthiourea as nitrification inhibitor. Bottles were sealed and prepared to capture generated carbon dioxide leading to a pressure drop proportional to the consumed oxygen, representing the biochemical oxygen demand (BOD). Samples were incubated for 90 days under stirring and in the dark, at 20 °C in a climate chamber. Biodegradability of the test substance was calculated with the BOD for complete biodegradation and the measured BOD value:

$$\text{BOD (mg O}_2\text{ per l)} = \text{mg polymer} \times \frac{\text{ThOD mg O}_2}{1 \text{ mg polymer}} \times \frac{1}{0.157 \text{ l water}}$$

$$\text{Biodegradability (\%)} = \frac{\text{BOD measured (mg O}_2\text{ per l)}}{\text{BOD for complete biodegradation (mg O}_2\text{ per l)}} \times 100$$

Results and discussion

Initially, a thermotolerance pre-screening was performed with cutinases identified through literature research. Preliminary thermotolerance tests were conducted at 100 °C, followed by another test with stepwise increases of 10 °C each between 100 °C and 200 °C with a PES polyol as substrate. Subsequently thermotolerance and cutinase incorporation tests were combined to investigate whether cutinase activation occurs after embedment within the PES polyol. Cutinase activity after heat treatment was measured based on pH changes caused by ester hydrolysis. Most promising cutinase candidates were evaluated for their ability to degrade TPUs upon external cutinase addition under laboratory conditions. TPU degradation was quantified by monomer release and four well performing cutinases were further used in melt extrusion experiments with the two TPUs, TPU 4 and TPU 5, at processing temperatures up to 210 °C. Degradation assays were performed under laboratory conditions (200 mM KPi, pH 8.0 at 37 °C), and adipic acid release was quantified. Finally, biodegradation studies were performed with activated sludge to evaluate TPU 5 degradation at close to application conditions. Furthermore, mechanical properties of TPU 4 and TPU 5 with embedded cutinases as well as cutinase distribution within

the two TPUs were analysed by fluorescence and PiFM measurements.

Selection of thermostable cutinases

TPUs are generally processed at temperatures ≥145 °C using extrusion and injection moulding,^{60–63} therefore, incorporated cutinases must be very thermostable. Initial heat stability tests were conducted for eleven cutinases that were identified by literature research; only polyesterases with high activities and a $T_m > 70$ °C were selected (Table S4). After cutinase expression, ester hydrolysis for all eleven cutinases was quantified using lyophilised crude clarified lysate with the photometric *p*-nitrophenyl butyrate (*p*NPB) assay; ester hydrolysis of HiC was in contrast to the other cutinases assessed with lyophilisate of the purified HiC. The *p*NPB assay confirmed activity for all cutinases with significant differences; HiC had the highest specific activity (Fig. S1). Following activity determinations, a preliminary thermotolerance test was performed, in which the cutinases were embedded into the molten PES polyol at 100 °C. In the thermotolerance test, lyophilised powders of clarified lysate and of purified HiC were employed to determine the extent of enhanced thermotolerance. Cutinases were investigated in their dry form as previous studies reported an improved thermotolerance of hydrolases in their dehydrated state,^{52,54,66} likely due to reduced structural flexibility, resulting in more rigid and stable hydrolase conformations. After heat treatment, hydrolysis activity of cutinases was determined in buffer at ambient temperature with the phenol red indicator (see methods part). Ester hydrolysis activity was confirmed for all incorporated cutinases and visible through a colour change from red to orange/yellow (Fig. S2). For HiC, SvCut190*SS, ThcCut1, ThcCut1-ACCG, and LCC-ICCG, acid release was detectable with the phenol red assay after 60 minutes with the ‘most intense’ signal for HiC. LCC wildtype and the WCCG variant showed a slower acid formation from PES polyol hydrolysis after 18 hours (Fig. S2a), whereas BhrPETase, DuraPETase^{N233K}, and TfCut2 had only a minor activity. These differences in hydrolysis activity against PES polyol align with the differences in the specific cutinase activities quantified with the *p*NPB assay (Fig. S2). Notably, incorporated cutinases can be activated by the surrounding aqueous medium, resulting in polymer hydrolysis from within the core of the PES polyol.

Thermotolerance of the five best-performing cutinases (HiC, ThcCut1, TheCut1-ACCG, SvCut190*SS, LCC-ICCG) were studied by PES polyol degradation after embedment at processing temperatures that were increased in 10 °C increments from 100 °C to 200 °C. Quantification of PES polyol degradation was subsequently performed in buffer at ambient temperature using an automated assay under pH-stat conditions employing the BioLector® Pro device. In detail, the PES polyol samples were incubated in aqueous buffer, while base titration was automatically conducted in the BioLector® Pro upon a decrease in pH caused by acid formation after ester hydrolysis. The total amount of consumed base served as a quantitative



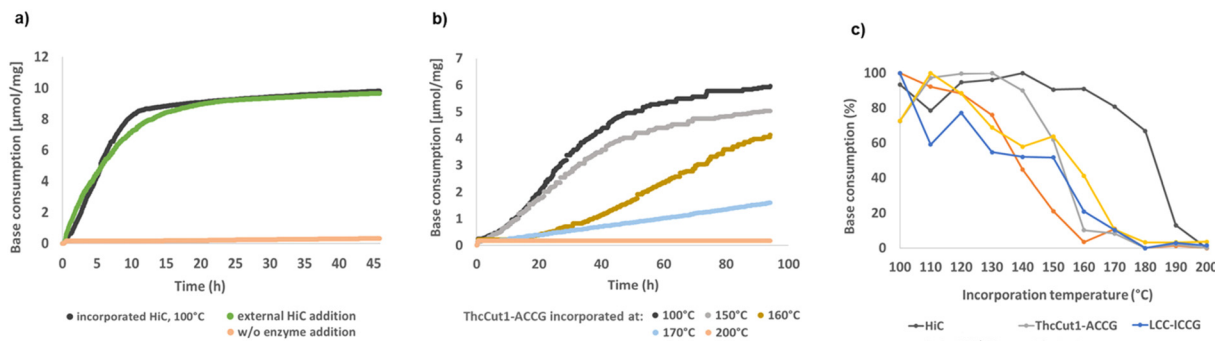


Fig. 1 Base consumption during enzymatic pre-screening assays under pH-stat (7.0) conditions using the BioLector® Pro micro-fermentation device. Assays were conducted with PES polyol containing (a) 0.1 wt% HiC, embedded at 100 °C, (b) 0.1 wt% ThcCut1-ACCG, embedded at 100 °C–200 °C, and (c) 0.1 wt% HiC, ThcCut1, ThcCut1-ACCG, SvCut190*SS or LCC-ICCG embedded at temperatures from 100 °C–200 °C. As reaction medium 100 mM KPi (+50 µg ml⁻¹ kanamycin), pH 7.0 was used. Base consumption is based on single measurements and in (c) the final base consumption has been normalized to the highest value for each cutinase individually.

measure for enzymatic ester hydrolysis. The assay could simultaneously be performed for 32 samples in flower plates.

Fig. 1a shows the base consumption of an initially analysed PES polyol sample containing HiC embedded at 100 °C. Both, the positive control with externally supplemented HiC and the sample with embedded HiC, exhibited similar high base consumption slopes. The negative control without HiC supplementation did show >95% less base consumption compared to that of both HiC-treated PES polyol samples. These results validate the BioLector® Pro pH-stat assay for studying differences in cutinase activity based on ester hydrolysis. Next, PES polyol samples containing one of the five cutinases (HiC, ThcCut1, ThcCut1-ACCG, SvCut190*SS, LCC-ICCG), embedded at temperatures from 100 °C to 200 °C, were subjected to the BioLector® Pro pH-stat assay. Fig. 1b exemplarily shows the base consumption of PES polyol samples with incorporated ThcCut1-ACCG over a period of 100 h at varied incorporation temperatures from 100 °C to 200 °C. Impact of incorporation temperature on activity of ThcCut1-ACCG is shown (Fig. 1b) and as a general trend it could be observed that incorporation temperatures above 150 °C result in significant reduced ThcCut1-ACCG hydrolysis.

In (Fig. 1c) the five cutinases (HiC, ThcCut1, ThcCut1-ACCG, SvCut190*SS, LCC-ICCG) were compared in their PES polyol hydrolysis performance after incorporation at varied processing temperatures that ranged from 100 °C to 200 °C. All five cutinases had a detectable hydrolysis activity up to a processing temperature of 170 °C (Fig. 1c). HiC outperformed the other cutinases, as base consumption was measurable in samples processed at 190 °C. Excitingly, ThcCut1, ThcCut1-ACCG, SvCut190*SS, and LCC-ICCG withstood melting processing temperatures between 150 °C to 170 °C.

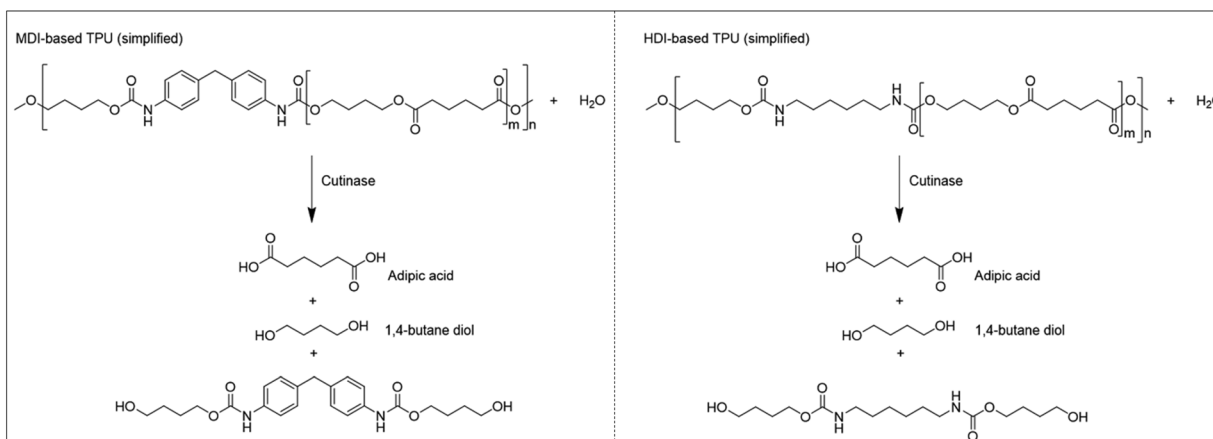
Enzymatic degradation of TPUs

TPUs represent a more challenging substrate for hydrolysis compared to the PES polyol, due to the presence of hard segments which are highly crystalline and non-flexible regions, thereby inhibiting the mobility of the polymer chains.^{6,67}

HiC was chosen for a screening of enzymatic degradability of different TPUs due to its outstanding thermotolerance matching standard TPU processing conditions. Five PES-TPUs (Table 1) were incubated with externally supplemented HiC (5% v/v; at 37 °C for 33 days). TPU degradation was quantified by the release of the water-soluble degradation product adipic acid through HPLC measurements (Scheme 1) applying a chromatographic separation method using a solvent gradient, as outlined in the materials section and Table S3. Besides quantification of one of the TPU degradation products, weight loss determinations and microscopic visualisations were conducted.

For two out of the five TPUs, significant adipic acid release was detected upon incubation with HiC. The highest hydrolysis was measured for TPU 5 with 46%, followed by 23% adipic acid release measured for TPU 4 after 33 days (Table S5). In detail, TPU degradation was detected starting from the first sample taken after 9 days. Adipic acid release correlated well with weight loss, which reached 38% for TPU 5 and 12% for TPU 4 (Table S5). The adipic acid release and weight losses for TPU 1–3 were in the range of the negative controls, indicating rather minor autohydrolysis than enzymatic degradation. As TPU 4 and TPU 5 have a higher ester bond content than TPU 1–3, the correlation between PES content and TPU 1–5 degradability by cutinases becomes evident from these results (Table 1). For both TPUs, TPU 4 and TPU 5, enzymatic degradation was also evident through optical surface changes (Fig. 2 and Fig. S3). HiC penetrated the TPU 4 granule, yielding a crumbly and porous surface (Fig. 2c and d). Surface images from light microscopy and SEM show many cracks on the HiC-treated TPU surfaces, while no visible changes occurred in the negative controls without HiC treatment (Fig. 2 and Fig. S3). Both TPUs, the aromatic TPU 4 and the aliphatic TPU 5, were chosen for further degradation studies with all five thermotolerant cutinases (HiC, ThcCut1, ThcCut1-ACCG, SvCut190*SS, LCC-ICCG). Cutinase concentrations varied from 0.1–1.0 wt% relative to the TPU weight and were initially probed for TPU 4 to select a suitable concentration for efficient degradation. Adipic acid release and





Scheme 1 Scheme of cutinase catalyzed ester hydrolysis of TPU (simplified) with resulting degradation products. Left part, top: methylene diphenyl diisocyanate (MDI) based TPU; right part, top: hexamethylene diisocyanate (HDI) based TPU. The aromatic urethane is found in TPU 1–4 (left), while the aliphatic urethane is found in TPU 5 (right). m, n : number of repeating units; lower part: TPU degradation products after cutinase catalyzed ester hydrolysis.

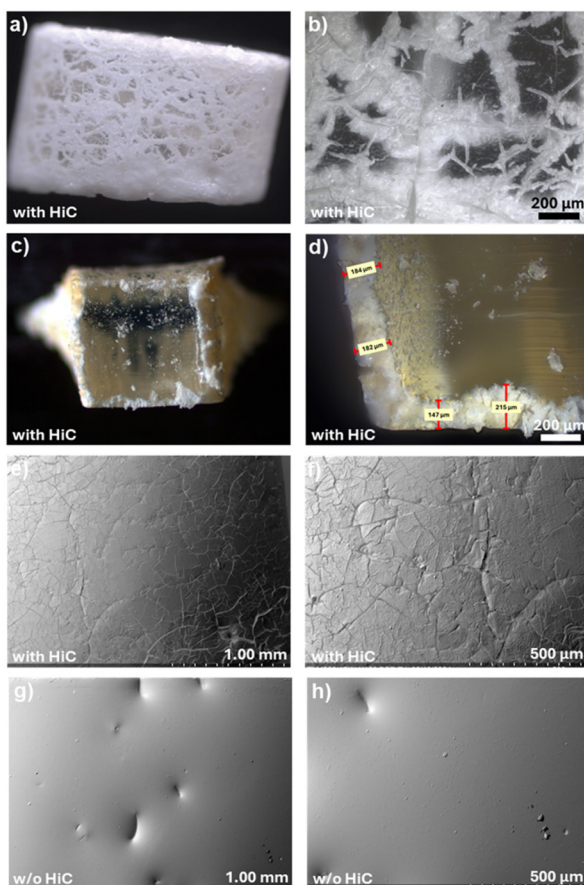


Fig. 2 Microscopic images of TPU 4 with and without (w/o) HiC treatment. The samples were incubated in KPi (200 mM, pH 8.0) for 33 days at 37 °C, with or without the addition of 5% (v/v) HiC. Light microscopy images show the surface of a TPU 4 granule treated with HiC at 25 \times (a) and 200 \times (b) magnification, and the cross-section at 25 \times (c) and 100 \times (d) magnification. SEM images display the surface of TPU 4 granules treated with HiC at 50 \times (e) and 100 \times (f) magnification, and without HiC treatment at 50 \times (g) and 100 \times (h) magnification.

weight loss were confirmed for all five cutinase loads ranging from 0.1–1.0 wt% (Table S6). To our knowledge, this is the first time that TPU degradation has been reported for SvCut190*SS, ThcCut1-ACCG, and LCC-ICCG. HiC, SvCut190*SS, ThcCut1, and ThcCut1-ACCG were the best-performing cutinases in respect to TPU 4 degradation; adipic acid release increased alongside with increasing cutinase load which confirms the cutinase-catalysed TPU degradation (Table S6). At the highest cutinase load of 1 wt%, 2.8–6.2% adipic acid release was detected. SvCut190*SS yielded the highest adipic acid release as well as the highest weight loss of 5.5% while in the negative control without cutinase supplementation the degradation was negligible (0.5% adipic acid release; 0.3% weight loss; Table S6). Degradation studies with TPU 5 revealed, as a general trend, that cutinase concentrations of 0.3 wt% and 0.5 wt% are sufficient to degrade TPU 4 with an adipic acid release of 2.6%–3.5% (or weight loss of 2.5%–3.5%) after 33 days without being limited in enzyme concentration. Subsequently, 0.3 wt% and 0.5 wt% were applied for all cutinases in comparable degradation studies for TPU 5. HiC resulted in the highest adipic acid release from TPU 5 among the evaluated cutinases, with up to 72% release at an enzyme load of 0.5 wt% (Fig. S4). The other cutinases achieved up to 29% adipic acid release from TPU 5 with an enzyme load of 0.5 wt% (by ThcCut1; Fig. S4). All five cutinases were able to degrade TPU 5 with LCC-ICCG yielding the lowest adipic acid release (2% at 0.3 wt% and 4% at 0.5 wt%; Fig. S4). Given that significant TPU degradation was verified for both 0.3 wt% and 0.5 wt% cutinase concentrations, 0.3 wt% was chosen for all heat-based incorporation experiments *via* melt extrusion since it proved to be sufficient for determining TPU degradation.

Enzymatic degradation of TPUs with extrusion embedded cutinases under *in vitro* conditions

After identifying enzymatically degradable TPUs and suitable cutinase candidates for the extrusion-based embedment, the

process was performed on a twin-screw micro-compounder, which mimics the technical compounding process required to produce innovative biodegradable biocomposite TPUs. The developed compounding process approaches large scale processes to ensure scalability of the developed process. Compounding was conducted within a temperature range of 150 °C to 200 °C to study the temperature limit for the four selected cutinases (HiC, ThcCut1-ACCG, SvCut190*SS, LCC-ICCG) with respect to TPU degradation activity for TPU 5. Whether TPU degradation was enhanced with embedded cutinase was investigated with varied processing temperatures. Additionally, here we embedded HiC into TPU 4 at tempera-

tures between 190 °C and 210 °C to determine the limiting processing temperature for HiC concerning TPU degradation activity. The produced cutinase-containing TPU samples were incubated in buffer to initiate hydrolytic cutinase activity after embedment. Cutinase activity was measured by adipic acid release upon incubation over three weeks, as well as through optical changes of the cutinase-degraded TPUs. Fig. 3 shows the adipic acid release from TPU samples with incorporated lyophilised crude clarified lysates of SvCut190*SS, ThcCut1-ACCG, and LCC-ICCG, as well as of purified HiC at varied processing temperatures. TPU degradation activity was confirmed for all incorporated cutinases by the release of adipic acid

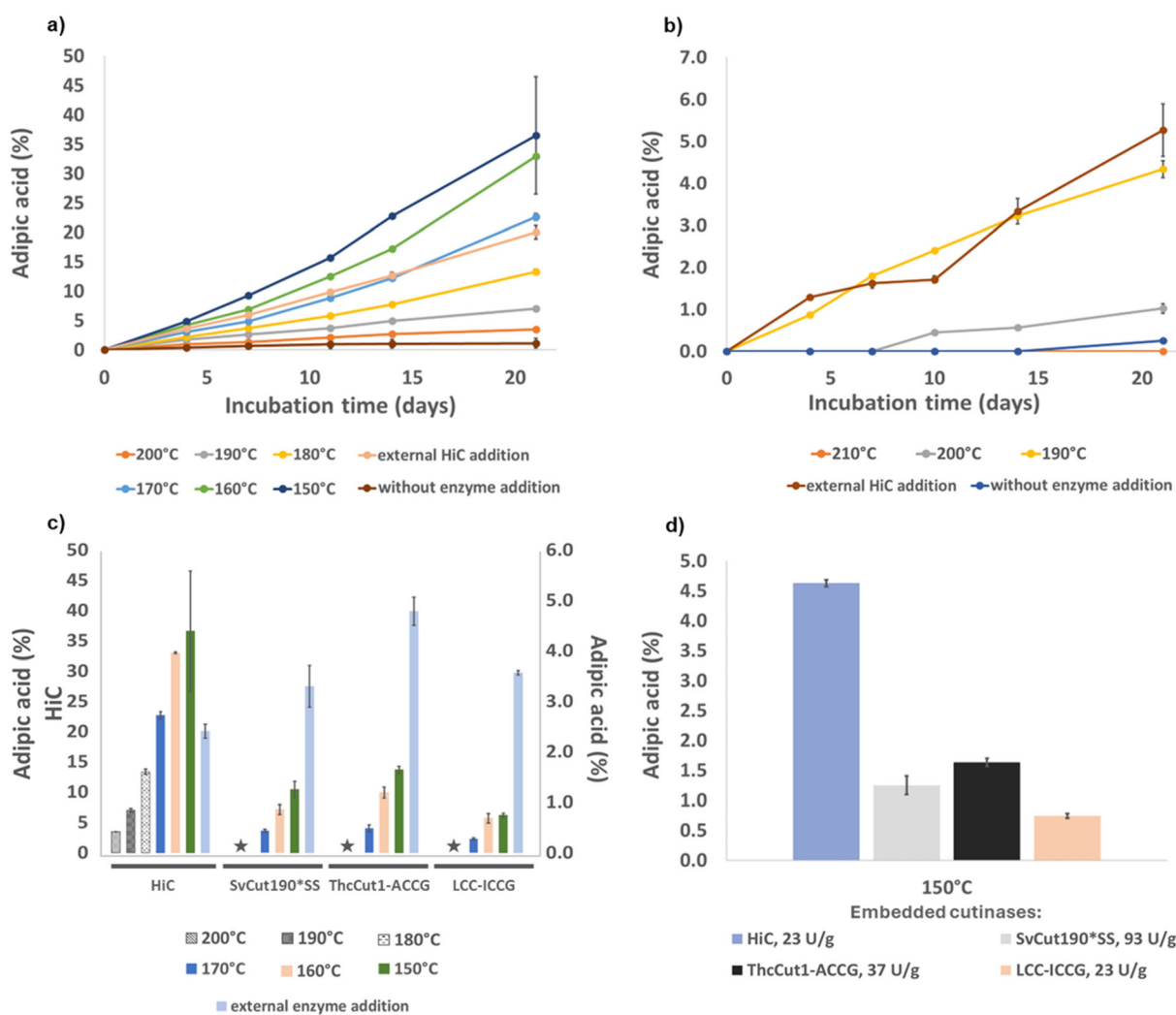


Fig. 3 Adipic acid release from TPU 4 and TPU 5 with melt extrusion-based incorporated cutinases. Incorporation temperatures are indicated. The degradation studies were performed at 37 °C in aqueous buffer (KPi, 200 mM, pH 8.0). The data is given as the means \pm standard deviations of triplicate reactions. All values measured with incorporated HiC were corrected by each corresponding autohydrolysis control without enzyme addition. All values measured with incorporated non-purified lysates were corrected by the empty vector control. Indicated U (units) represent the incorporated cutinase activity in pNPB U per g TPU. TPU without or with external cutinase addition was extruded at 180 °C. Adipic acid release from (a) TPU 5 and (b) TPU 4 with 0.3 wt% (\pm 197 pNPB U per g TPU) incorporated HiC. (c) Adipic acid release from TPU 5 after 21 days of incubation with 0.3 wt% incorporated HiC, or SvCut190*SS, ThcCut1-ACCG, and LCC-ICCG lysates. Data for lysate samples processed at 180 °C–200 °C is not shown, as the values for the empty vector control exceeded the adipic acid release from cutinase containing TPU after 21 days (indicated by \star). (d) Adipic acid from TPU 5 after 21 days of incubation with incorporated HiC, normalized to 23 pNPB Units per g TPU, and incorporated SvCut190*SS, ThcCut1-ACCG, and LCC-ICCG lysates.



from TPU 5 upon one week of incubation in an aqueous buffer at 37 °C (Fig. 3). As a general observation, ThcCut1-ACCG, LCC-ICCG, and SvCut190*SS, degradation activity could be confirmed for TPU 5 up to a processing temperature of 170 °C (Fig. 3c). From these three cutinases the highest adipic acid release with a value of 1.6% was measured for embedded ThcCut1-ACCG after 21 days of TPU 5 incubation. SvCut190*SS led to 1.3% and LCC-ICCG to 0.7% adipic acid release, after the same incubation time. The latter values resulted from TPU 5 samples processed at 150 °C. Interestingly, at a processing temperature of 180 °C adipic acid release could be measured after 11 days in TPU 5 containing one of the three cutinases (ThcCut1-ACCG, LCC-ICCG, and SvCut190*SS); at this time, no adipic acid was detected in either control sample, TPU without cutinase treatment, or TPU with incorporated empty vector lysate. Surprisingly, after 21 days, substantial adipic acid release from the control sample with incorporated empty vector lysate could be measured. A similar trend was also observed in the heated negative controls without enzyme addition, which indicates autohydrolysis. HiC retained TPU 4 and TPU 5 hydrolysis activity even after being embedded at a processing temperature of 200 °C, as again quantified by HPLC analysis of adipic acid releases (1.0% for TPU 4; 3.5% for TPU 5; Fig. 3a and b). Even at this high processing temperature, the release of adipic acid was improved more than threefold compared to the negative controls for both TPUs. The fact, that HiC retained measurable hydrolysis activity after compounding at 200 °C in both TPUs is significant, given that elevated temperatures are often required to achieve homogenous additive dispersion within the melt phase during TPU compounding. At an incorporation temperature of 150 °C, the adipic acid release of TPU 5 with embedded HiC was 32-fold higher compared to the TPU 5 without cutinase treatment, corresponding to 36.5% of adipic acid. Compared to externally supplemented HiC an almost twofold higher hydrolysis kinetic could be achieved with equimolar concentrations of embedded HiC (Fig. 3a). In essence, incorporation of lyophilised HiC outperforms externally supplemented HiC, which is a first proof of concept that TPU degradation can overall be accelerated through cutinase embedment and is from the point of view of the authors an important achieved milestone towards TPU polymers designed for degradation. An additional set of experiments with HiC was performed to confirm the superior thermostability properties and TPU degradation activity of HiC based on incorporated activity units per gram TPU (Fig. 3d). So far, incorporated cutinases were added at equal masses (0.3 wt%) regarding the cutinase preparation, partially based on lyophilised crude lysate. As an exception, HiC appeared to be a relatively pure commercial protein preparation likely containing more cutinase than the prepared crude lysates. As this enzyme outperformed all other cutinases, it was evaluated to what extent this is based on merely a higher enzyme concentration. Therefore, the concentration of HiC was normalized based on *p*NPB activity units to the lowest incorporated cutinase activity so far (23 *p*NPB U per g TPU; Table S2), which is comparable to the activity of the previously incorporated

LCC-ICCG. HiC performs as expected, also normalized on activity, superior to the LCC-ICCG and also to the ThcCut1-ACCG and SvCut190*SS, which both were incorporated with higher activities than HiC (Fig. 3d). Adipic acid release from TPU 5 with incorporated normalized HiC was three- to sixfold higher compared to TPU 5 containing the other three cutinases (Fig. 3d). Cutinase embedment leads to TPU degradation from within the material until cutinase is released from the polymer and accelerates degradation also on the surface (see kinetics Fig. 3a). The extent of degradation is visually observable through cavities and morphological changes on the surface of TPU 5 samples, shown in Fig. 4 and Fig. S5. Samples containing embedded HiC exhibited extensive cracks with a rocky surface and a whitish/opaque appearance caused by HiC-degraded TPU 5 (Fig. 4c and d). The positive control, in which HiC was only externally supplemented, is degraded at the surface, while the interior of the sample remains clear and unaffected (Fig. 4e and f). The latter observation shows that in

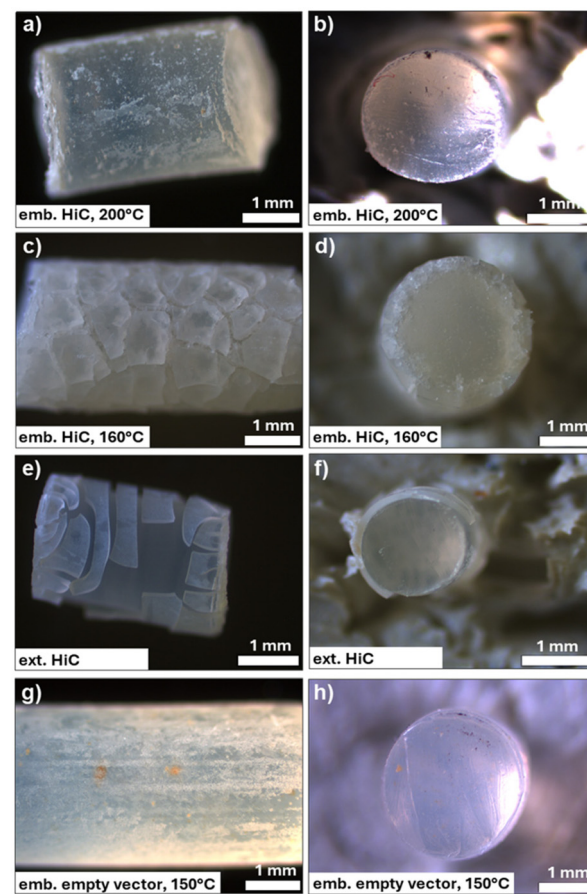


Fig. 4 Microscopic images of TPU 5 after 21 days incubation at 37 °C in KPi (200 mM, pH 8.0). Samples contained embedded (emb.) or externally added (ext.) HiC (a–f) or embedded pET26b_EV (g, h) lysate, all in a concentration of 0.3 wt%. HiC and empty vector incorporation was realized via melt extrusion at the indicated temperatures. The TPU for external HiC addition was molten at 180 °C, before enzyme treatment. (a), (c), (d) and (e) TPU granule surface, (b), (d), (e) and (f) TPU granule cross-section, all at 25 \times magnification at darkfield.



the positive control with externally added HiC, TPU 5 was degraded from the surface, whereas with incorporated HiC, degradation in bulk occurred from within the TPU 5. In summary, the obtained degradation results show that HiC is the best-performing cutinase with the highest thermostability during the extrusion process. To evaluate whether this exceptional activity is due to high cutinase purity, which is not given for the lyophilised lysates, an additional experiment was conducted to compare differences in hydrolytic activity and thermostolerance between purified and non-purified cutinase. As for HiC only the already purified form was available, SvCut190*SS was chosen for this comparison since it already demonstrated relevant thermostolerance and TPU degradation in its non-purified form. The IMAC-purified SvCut190*SS was incorporated into TPU 5 *via* melt extrusion, with the concentration normalized to match that of the non-purified SvCut190*SS from lyophilised crude lysate. The subsequent degradation study revealed higher thermostolerance of the purified SvCut190*SS, as adipic acid release was detected even in TPU 5 samples processed at 200 °C. In contrast, for samples with non-purified SvCut190*SS, an incorporation temperature of 180 °C was the limit at which adipic acid release was measurable (Fig. S6). Furthermore, the overall released adipic acid amount was nearly twofold higher in samples with embedded purified SvCut190*SS (170–180 °C) compared to the non-purified lysate, which aligns with previously observed results with purified HiC. The results confirmed that at TPU-relevant processing temperatures a superior hydrolysis activity can be achieved with purified cutinases compared to lyophilised crude cutinase preparations. In summary, the *in vitro* degradation studies conducted on various TPU/cutinase combinations demonstrated that melt extrusion-based cutinase embedment represents a feasible approach for the development of degradable TPUs – particularly relevant in application areas where conventional recycling is impractical, such as in agriculture and forestry.

Differential scanning calorimetry of cutinase containing TPU

It is generally known that polyester-cleaving enzymes exhibit a preference for hydrolysing the amorphous domains of semi-crystalline polyesters such as PET,⁶⁸ PCL,⁶⁹ and PU.³⁵ Soft segments within the TPU are generally formed by amorphous polyesters,^{2,5,7,8} which are expected to be the preferred hydrolysis targets for cutinase-catalysed degradation. Differential scanning calorimetry (DSC) measurements were used to evaluate differences in crystallinity of the soft and hard segments in the TPU 5 samples; goal is to study if hydrolysis also occurred in crystalline regions of the polyester segment. In the latter case, a decrease in crystallinity in the soft segments is expected in the HiC-containing TPU 5, as ester hydrolysis was already verified by adipic acid release. Results obtained with the DSC measurements are in line with the so far observed enzymatic degradation of TPU 5. A significant decrease in the crystalline polyester part of 54% was measured for the soft segments of TPU 5, containing HiC, incorporated at 150 °C compared to the non-heated negative control without a cutinase (Fig. S7).

Obtained reduction can likely be attributed to degradation of the crystalline polyester within the soft segments. Interestingly, an increase by 75% in the crystalline hard segments was observed in the same HiC-containing TPU sample, compared to the negative control. The melting curve for the positive control, in which HiC was supplemented externally during the degradation study, was similar to that of the empty vector and negative control (Fig. S7a).

Biodegradation of extruded TPU granules with embedded cutinases

After it was proven that cutinase incorporation into TPU enables the degradation into monomers, the biodegradation of cutinase-containing TPU 5 was investigated in a relevant natural environment. Activated sludge from a wastewater treatment plant according to the OECD 301 F guideline was selected as biodegradation trial close to application conditions.

Several control samples were studied in the degradation test to evaluate different aspects during the biodegradation process. One negative control was TPU 5 with incorporated empty vector lysate to investigate potential background activity from other cell components present in the incorporated non-purified lysates (ThcCut1-ACCG, SvCut190*SS, LCC-ICCG). Another negative control was prepared by embedding bovine serum albumin (BSA) into TPU 5 to mimic hydrolytically inactive protein. This control aimed to evaluate whether denatured proteins could potentially serve as a nutrient source for micro-organisms, resulting in enhanced oxygen consumption due to the metabolism of proteins rather than PU monomers. Both controls showed similar results to TPU 5 without any additive-treatment (original TPU; 3.5%), with 5.1% (empty vector) and 5.0% (BSA) biodegradation respectively (Fig. 5 and Fig. S8). This shows that both controls did not significantly boost biodegradation. The biodegradation of TPU 5 with embedded cutinases is represented in Fig. 5 and Fig. S8. The

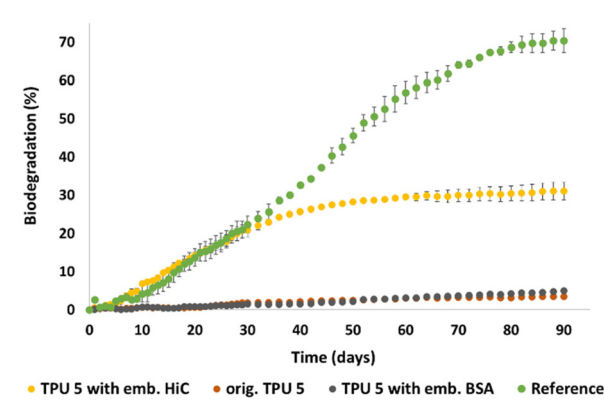


Fig. 5 Biodegradation of TPU 5 with 0.3 wt% HiC, embedded (emb.) at 150 °C. The degradation study was conducted according to OECD 301 F with activated sludge. Original (orig.) TPU 5 before melt extrusion and TPU 5 with 0.3 wt% incorporated BSA served as negative controls. As reference, cellulose was used. Biodegradation was monitored by the microbial oxygen demand over a period of 90 days at 20 °C.



results demonstrate that TPU 5 with embedded HiC exhibited a remarkable final biodegradation of 31.1% (Fig. 5), while ThcCut1-ACCG, SvCut190*SS, LCC-ICCG yielded a final biodegradation of TPU 5 between 4.7–6.0% (Fig. S8). The high biodegradation of TPU 5 with embedded HiC indicates that HiC is particularly effective in hydrolysing the polyester region of the TPU, leading to the release of oligomers and monomers, such as adipic acid, known to be readily biodegradable,⁷⁰ which are subsequently mineralized by the microorganisms present in the activated sludge. The accelerated biodegradation with HiC is evident from the steeper slope observed after 5–7 days of incubation, suggesting efficient enzymatic activity facilitating TPU mineralization. This also supports the hypothesis that the initial depolymerization of plastics into oligomeric and monomeric structures represents a bottleneck in biodegradation. During the initial 30 days, the biodegradation of TPU 5 containing HiC matched that of the cellulose reference, further validating the efficacy of HiC in accelerating biodegradation compared to TPU 5 without cutinase treatment (Fig. 5). After that period, a slower biodegradation was observed, necessitating further studies to understand the underlying cause. Summarizing the findings from the biodegradation study with cutinase-containing TPU 5, the previously described improved degradation of that material under *in vitro* conditions was confirmed by significantly accelerated biodegradation, highlighting that ester hydrolysis leads to enhanced biodegradation, whereas TPU without additional cutinase treatment underwent negligible decomposition. These findings are in line with other published results demonstrating a significant improvement in the biodegradation of enzyme-containing polymers. One study reported for example that PLA films containing an engineered PLAase, incorporated *via* melt extrusion at 160 °C, completely decomposed within 24 weeks at 28 °C in compost soil.⁵³ Another study reported biodegradation rates of 66%, 81%, and 98% for PCL, PBS, and PBSA, respectively, in seawater, with extrusion-based incorporated HiC.⁵⁴

Since long-term stability of embedded cutinases is crucial for TPU degradation performance, we addressed this point by conducting an additional activated sludge biodegradation study after eight months of TPU storage. TPU 5 with ThcCut1-ACCG embedded at 170 °C exhibited a biodegradation rate comparable to the initial data, reaching 9% after 90 days, thereby demonstrating high cutinase stability over prolonged storage (Table S7).

Overall, the reported findings demonstrate, that ester hydrolysis can be a rate limiting step in PES-TPU biodegradation, which can be overcome by cutinase incorporation. The initial ester hydrolysis significantly accelerated TPU biodegradation, by releasing readily biodegradable monomers such as adipic acid⁷⁰ and enabled the usage of TPU as sole carbon source.

These findings confirm application opportunities of incorporated cutinases for accelerated TPU biodegradation in environments close to application conditions, especially when recycling is not an option.

Cutinase distribution after extrusion-based incorporation into TPUs

A homogeneous cutinase distribution within the TPU is important to achieve a rapid TPU degradation. Fluorescent microscopy was employed to evaluate how homogenously HiC has been distributed through the extrusion process. From the fluorescent microscopy image of TPU 5 with fluorescent-labelled incorporated HiC, agglomerates that emit a fluorescent signal are visible, likely indicating HiC presence (Fig. 6a). No such signal was observed in the TPU 5 without incorporated HiC (Fig. 6b). Fluorescent agglomerates are evenly detectable over the sample slice, indicating a homogenous HiC distribution (Fig. 6a).

Photo-induced force microscopy (PiFM) was applied to further clarify the chemical nature of these particles. In order to validate how general applicable a well-dispersed cutinase distribution could be achieved the cutinase SvCut190*SS was also incorporated within TPU 4 and TPU 5. The topography of both TPUs was examined, along with mapping each of the two incorporated cutinases, HiC and SvCut190*SS, on the surface of the TPU samples. Reference measurements showed that TPU 4 and TPU 5 without embedded cutinases exhibited carbonyl (C=O) stretching vibrations at 1730 cm⁻¹, characteristic for PES, while the amide I vibration at a wavenumber of 1640 cm⁻¹, which is an indicator for protein presence, was

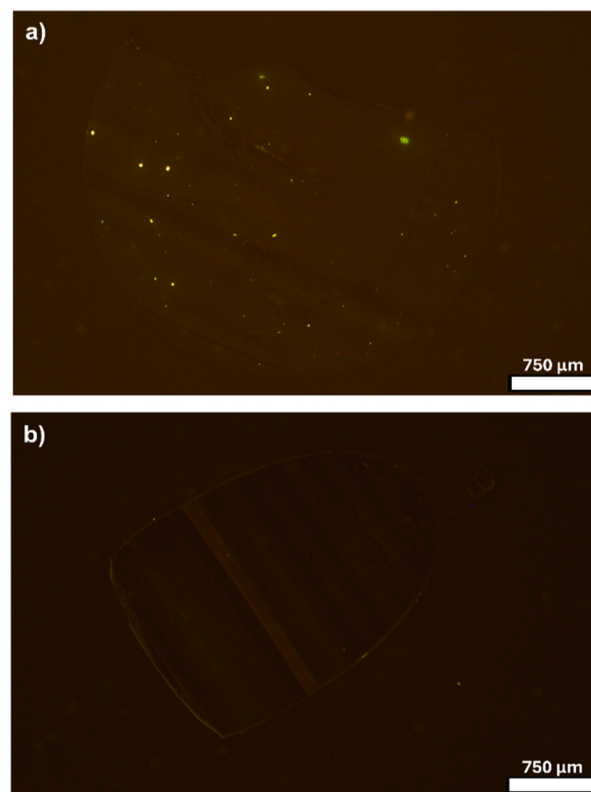


Fig. 6 Fluorescence microscopy image of microtome cuts of (a) TPU 5 with embedded NHS-fluorescein labeled HiC and (b) TPU 5 without embedded cutinase. Cutinase incorporation was performed at 150 °C at a concentration of 0.3 wt% HiC.



absent (Fig. S9). These measurements served as the basis for identifying cutinases within TPU 4 and TPU 5. In both, TPU 4 and TPU 5 with embedded HiC or SvCut190*SS, elevations on the surface were observed in the topographic PiFM images that distinguish themselves from the surrounding TPU area (Fig. 7a, Fig. S10a, S11a, and c). These agglomerates show higher absorption at a wavenumber of 1640 cm^{-1} compared to the surrounding area (Fig. 7b, Fig. S10b, S11b and d) and lower absorption when excited with a wavenumber of 1730 cm^{-1} (Fig. 7c and Fig. S10c). The PiFM spectrum confirmed the stretching of the amide I bond in these specific agglomerates evidencing the presence of protein, whereas the spectrum of a spot with higher absorption at 1730 cm^{-1} lacks this amide stretching (Fig. 7b, c and Fig. S1). Similar observations were made for TPU 5, but the agglomerates in TPU 5 samples are generally smaller compared to those in TPU 4, suggesting a finer distribution of the cutinase preparation during the incorporation process (Fig. S11). This might be attributed to the differences in T_m of both TPUs, with TPU 5 having a lower T_m , making it less viscous at the same processing temperature compared to TPU 4, thus facilitating better distribution of cutinase. In essence PiFM confirmed that fluorescent agglomerates observed in Fig. 6a are proteins and are

overall well-dispersed as shown for HiC and SvCut190*SS in the PiFM images (Fig. 7b, Fig. S10 and S11).

Mechanical properties of TPUs with embedded cutinases

Whether incorporation of cutinases affect mechanical properties of TPU 4 and TPU 5 was investigated to evaluate that the TPU-biocomposite can still meet the high requirements for the material properties set for a TPU in applications. Mechanical properties were studied with TPUs with and without embedded HiC or ThcCut1-ACCG as summarized in Table 2. TPU samples were prepared using 0.3 wt% purified HiC or non-purified ThcCut1-ACCG lyophilisates for extrusion-based incorporation as this concentration previously yielded sufficient results with regards to TPU degradation efficiency and evenly cutinase distribution within the TPU.

Tensile strength was highest in TPU samples without embedded cutinases and reduced by up to 43% in TPU 4 with embedded HiC. These results align with previous studies reporting tensile strength reductions of 46% in PCL and 25% in PBSA upon incorporation of 0.07% CalB (lipase B from *Candida antarctica*)⁶⁶ as well as a 39% reduction in PCL containing 0.02% HiC.⁵⁴ In TPU 5, the tensile strength differences between samples with and without embedded HiC or

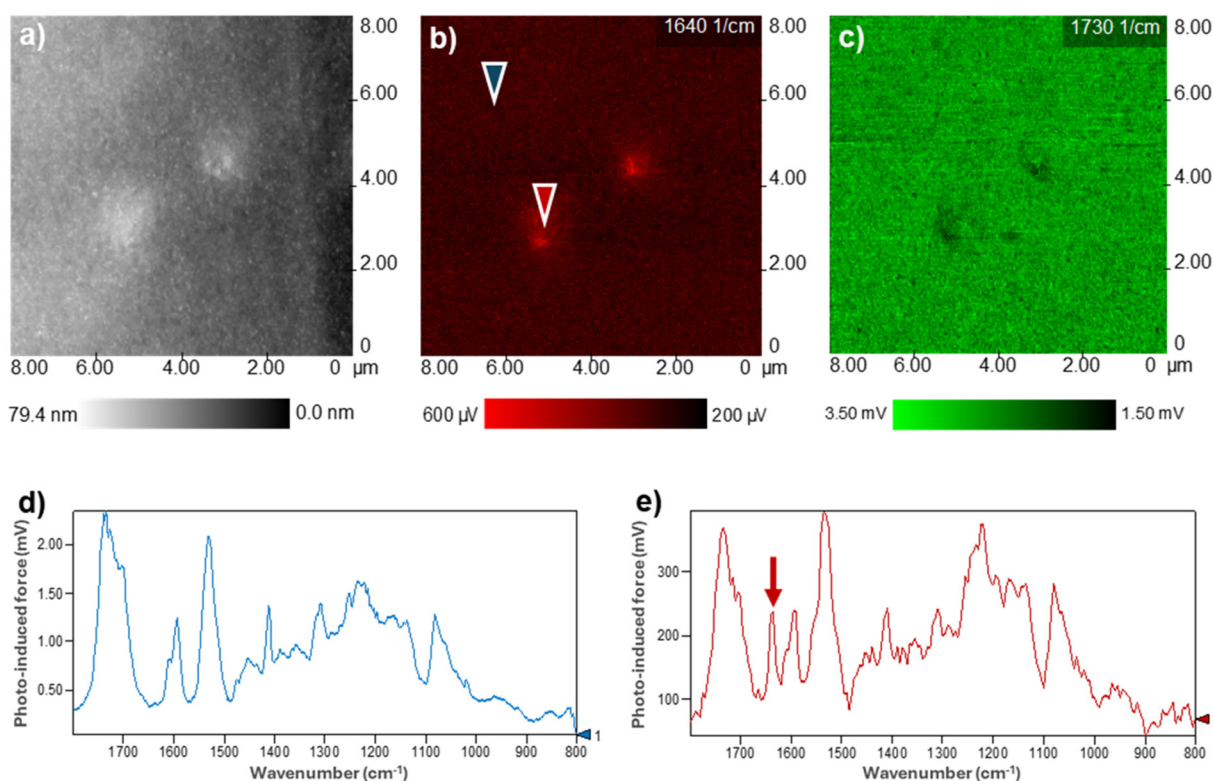


Fig. 7 PiFM images and spectra of TPU 4 with incorporated HiC. Cutinase incorporation was done at $200\text{ }^\circ\text{C}$ at a concentration of 0.3 wt%. (a) Topographic image, and (b, c) optical images at a wavenumber of (b) 1640 cm^{-1} (amide I stretching), and (c) 1730 cm^{-1} (carbonyl stretching, characteristic for polyester). Brighter areas in the topographic image indicate an elevation on the surface. In the optical images brighter areas indicate higher, and darker areas indicate lower absorption for the specific molecular composition, at each wavelength. PiFM spectra are displayed for (d) blue arrow location from (b) without amide I vibration, and (e) red arrow location from (b) with amide I vibration at 1640 cm^{-1} , indicating protein presence.

Table 2 Mechanical properties and kinematic solution viscosity of original TPU 4 and TPU 5 before melt extrusion, as well as TPU 4 and TPU 5 with and without incorporated HiC or ThcCut1-ACCG, after melt extrusion. Cutinase load was 0.3 wt%. n.d.: not determined

TPU	Processing temperature (°C)	Cutinase	Tensile strength (N mm ⁻²)	Elongation at break (%)	Solution viscosity (mm ² s ⁻¹)
4	No treatment	—	n.d.	n.d.	1.525
4	210	—	28.1 ± 2.4	604 ± 78	1.412
4	210	HiC	16.0 ± 1.3	702 ± 17	1.285
4	210	ThcCut1-ACCG	19.8 ± 1.0	671 ± 2	1.313
5	No treatment	—	n.d.	n.d.	1.384
5	180	—	25.5 ± 0.6	768 ± 19	1.378
5	180	HiC	25.4 ± 1.0	753 ± 23	1.374
5	180	ThcCut1-ACCG	24.6 ± 0.3	737 ± 6	1.367

ThcCut1-ACCG were negligible (Table 2). Although the cutinases are well-dispersed (Fig. 6a), their incorporation may interfere with TPU structure, which is well-tolerated by some TPUs without notable changes in mechanical properties, whereas others are impacted to some extent. The impact on tensile strength may be mitigated by decreasing the concentration of embedded cutinase without compromising the efficiency of TPU degradation.

Conclusions

In this study we successfully demonstrated the hydrolysis activity of five different cutinases on both aliphatic and aromatic TPUs. Additionally, we explored various conditions for the heat-based incorporation of four cutinases into TPUs, at processing temperatures up to 200 °C. All cutinases remained active up to at least 170 °C, with HiC exhibiting exceptional thermotolerance up to a processing temperature of 200 °C, enabling its incorporation into a wide range of TPUs. HiC-containing TPU 5 demonstrated a 32-fold higher adipic acid release compared to TPU 5 without cutinase treatment, and a 1.6–1.8 higher release compared to externally added HiC. These results demonstrate a first proof of concept that cutinase embedment into TPUs through melt extrusion can efficiently accelerate degradation which is an important milestone towards the design of biodegradable TPUs.

Responsible for the excellent TPU 5 (and TPU 4) degradation are the well-dispersed cutinases confirmed with fluorescent and PiFM imaging.

Throughout our work, we demonstrated TPU degradation by the detection of adipic acid as a main degradation product. In future studies it would be interesting to analyse other compounds resulting from TPU degradation.

Besides *in vitro* degradation studies in buffer, application potentials of cutinase-containing TPU were investigated by simulating environmental degradation conditions according to the highly recognized OECD 301 F guideline with diluted activated sludge at 20 °C. The studies yielded an almost ninefold accelerated biodegradation of TPU 5 with incorporated HiC compared to TPU 5 without additional HiC treatment. Unlike previous studies, which primarily investigated PU degradation under industrial composting conditions (45–58 °C) and still reported limited mineralisation of less than 30%,^{22–25} this

work describes over 30% biodegradation after 90 days under less favourable biodegradation conditions (20 °C, lower density of microorganisms). This demonstrates that cutinase incorporation can be a key-factor in the design for degradation of TPUs. These results are a promising foundation with regards to TPU 4 and TPU 5 being potentially used for applications in the agricultural and forestry sector, in which biodegradability is desired, as collection and recycling is not an economically viable option. Developing a new type of biodegradable TPU, particularly for applications where the end-of-life state is intended to be in nature, or items that end up in nature due to usage and weathering, like bristles for sweeping brushes, is of high interest for a sustainable polymer economy of TPUs in general.

Considering that for instance, the hydrolysis product adipic acid is known to be readily biodegradable in soil,⁷⁰ makes the reported results promising with regards to a nearly complete biodegradation of enzymatically treated TPU triggered by initial cutinase activity. By this, the reported method for cutinase incorporation into TPU represents a green advance towards reducing persistent TPU and a contribution to a circular PU economy. While the complete degradation of TPUs can effectively prevent waste accumulation, it also results in the release of aliphatic and aromatic amines, the latter of which raises environmental concerns due to their toxicity.^{71–73} However, microorganisms such as *Pseudomonas* sp. and *Cladosporium* sp. are known to metabolize aromatic amines such as 2,4-diaminotoluene and 4,4'-methylenedianiline and thereby contribute to the removal of these substances from the environment.^{74,75}

Since PU biodegradation is highly dependent on the environment, the microorganisms present, and the polymer-degrading enzymes found there, the presented approach offers a method that makes the decomposition less reliant on varying environmental conditions, by already providing biodegradation catalysts.

The validated TPU degradation concept represents from the point of view of the authors an important step to advance TPU into a green polymer as part of a circular TPU economy.

Author contributions

Daniela Knopp: project administration; investigation; validation; visualization; data curation; formal analysis; method-



ology; writing – original draft. Simone Göbbels: investigation; methodology. René Münchrath: investigation. Cristina Lavilla Aguilar: investigation; validation. Michael Kessler: conceptualization; resources. Qi Chen: investigation; data curation; visualization. Marian Bienstein: conceptualization. Linda Katharina Wiedemann, Jonas Gerund, and Edward Zoet: investigation; visualization. Gernot Jäger: conceptualization. Ulrich Schwaneberg: conceptualization; supervision. Lukas Reisky: funding acquisition; conceptualization; supervision; project administration. All: writing – review & editing.

Conflicts of interest

The authors Daniela Knopp, Simone Göbbels, René Münchrath, Cristina Lavilla Aguilar, Michael Kessler, Qi Chen, Linda Katharina Wiedemann, Jonas Gerund, Edward Zoet, Gernot Jäger and Lukas Reisky are employees of Covestro. Patent applications have been filed.

Data availability

The data supporting this article have been included as part of the supplementary information (SI). Supplementary information is available. See DOI: <https://doi.org/10.1039/d5gc03512k>.

Acknowledgements

We would like to thank Gudrun Schmidt for her consulting in the TPU extrusion processes. We also thank Dr Anne Fischer for analytical support and insightful discussions. Additionally, we thank Dr Stefanie Spindler for providing the FTIR data. We also thank Ton Brooijmans for providing the GPC data. We thank the German Federal Ministry of Research, Technology and Space (BMBFTR) for research funding (031B1272).

References

- 1 H. W. Engels, H. G. Pirkl, R. Albers, R. W. Albach, J. Krause, A. Hoffmann, H. Casselmann and J. Dormish, *Angew. Chem., Int. Ed.*, 2013, **52**, 9422–9441.
- 2 J. O. Akindoyo, M. D. H. Beg, S. Ghazali, M. R. Islam, N. Jeyaratnam and A. R. Yuvaraj, *RSC Adv.*, 2016, **6**, 114453–114482.
- 3 O. Bayer, *Angew. Chem.*, 1947, **59**, 257–272.
- 4 J. R. Fried, in *Polymer Science and Technology*, Prentice-Hall, PTR, Englewood Cliffs, NJ, 1995.
- 5 A. Loredo-Treviño, G. Gutiérrez-Sánchez, R. Rodríguez-Herrera and C. N. Aguilar, *J. Polym. Environ.*, 2012, **20**, 258–265.
- 6 G. T. Howard, *Int. Biodeterior. Biodegrad.*, 2002, **49**, 245–252.
- 7 R. J. Young and P. A. Lovell, *Introduction to Polymers*, CRC Press, Boca Raton, FL, 3rd edn, 2011.
- 8 M. Urgun-Demirtas, D. Singh and K. Pagilla, *Polym. Degrad. Stab.*, 2007, **92**, 1599–1610.
- 9 S. Research, Polyurethane Market Size, Share & Trends Analysis Report By Product (Flexible Foam, Rigid Foam, Coating, Elastomer), By End-User (Construction, Household Products, Transportation Equipment, Electronics) and By Region (North America, Europe, APAC, Middle East and Africa, LATAM) Forecasts, 2025–2033, <https://straitsresearch.com/report/polyurethane-market>, 2024, (accessed: 13th February, 2025).
- 10 A. Raczyńska, A. Góra and I. André, *Biotechnol. Adv.*, 2024, **77**, 108439.
- 11 M. Cregut, M. Bedas, M. J. Durand and G. Thouand, *Biotechnol. Adv.*, 2013, **31**, 1634–1647.
- 12 J. Datta, P. Kopczyńska, D. Simón and J. F. Rodríguez, *J. Polym. Environ.*, 2018, **26**, 166–174.
- 13 A. Kemon and M. Piotrowska, *Polymers*, 2020, **12**, 1752.
- 14 N. Mahajan and P. Gupta, *RSC Adv.*, 2015, **5**, 41839–41854.
- 15 I. Wojnowska-Baryła, K. Bernat and M. Zaborowska, *Int. J. Environ. Res. Public Health*, 2022, **19**, 13223.
- 16 M. S. Reddy, S. Basha, S. Adimurthy and G. Ramachandraiah, *Estuarine, Coastal Shelf Sci.*, 2006, **68**, 656–660.
- 17 L. Frère, I. Paul-Pont, J. Moreau, P. Soudant, C. Lambert, A. Huvet and E. Rinnert, *Mar. Pollut. Bull.*, 2016, **113**, 461–468.
- 18 A. Turner and K. S. Lau, *Mar. Pollut. Bull.*, 2016, **112**, 265–270.
- 19 V. Bauchmüller, M. Carus, R. Chinthapalli, L. Dammer, N. Hark, A. Partanen, P. Ruiz and S. Lajewski, *BioSinn – Products for which biodegradation makes sense*, <https://renewable-carbon.eu/publications/product/biosinn-products-for-which-biodegradation-makes-sense-pdf/>, 2021, (accessed: 21st December 2022).
- 20 A. Magnin, E. Pollet, V. Phalip and L. Avérus, *Biotechnol. Adv.*, 2020, **39**, 107457.
- 21 M. Rutkowska, K. Krasowska, A. Heimowska, I. Steinka and H. Janik, *Polym. Degrad. Stab.*, 2002, **76**, 233–239.
- 22 U. Zafar, A. Houlden and G. D. Robson, *Appl. Environ. Microbiol.*, 2013, **79**, 7313–7324.
- 23 L. Genovese, M. Soccio, M. Gigli, N. Lotti, M. Gazzano, V. Siracusa and A. Munari, *RSC Adv.*, 2016, **6**, 55331–55342.
- 24 P. Kucharczyk, A. Pavelková, P. Stloukal and V. Sedlarík, *Polym. Degrad. Stab.*, 2016, **129**, 222–230.
- 25 E. F. Gómez, X. Luo, C. Li, F. C. Michel and Y. Li, *Polym. Degrad. Stab.*, 2014, **102**, 195–203.
- 26 Commission Regulation (EU), 2023/2055 of September 2023, amending Annex XVII to Regulation (EC) No 1907/2006 (REACH) as regards synthetic polymer microparticles, *Off. J. Eur. Communities: Legis.*, 2023, **239**, 67–88.
- 27 J. Álvarez-Barragán, L. Domínguez-Malfavón, M. Vargas-Suárez, R. González-Hernández, G. Aguilar-Osorio and H. Loza-Tavera, *Appl. Environ. Microbiol.*, 2016, **82**, 5225–5235.
- 28 T. Nakajima-Kambe, Y. Shigeno-Akutsu, N. Nomura, F. Onuma and T. Nakahara, *Appl. Microbiol. Biotechnol.*, 1999, **51**, 134–140.



29 Y. Matsumiya, N. Murata, E. Tanabe, K. Kubota and M. Kubo, *J. Appl. Microbiol.*, 2010, **108**, 1946–1953.

30 S. J. Stachelek, I. Alferiev, H. Choi, C. W. Chan, B. Zubiate, M. Sacks, R. Composto, I.-W. Chen and R. J. Levy, *J. Biomed. Mater. Res., Part A*, 2006, **78A**, 653–661.

31 M. Osman, S. M. Satti, A. Luqman, F. Hasan, Z. Shah and A. A. Shah, *J. Polym. Environ.*, 2018, **26**, 301–310.

32 Y.-H. Peng, Y.-h. Shih, Y.-C. Lai, Y.-Z. Liu, Y.-T. Liu and N.-C. Lin, *Environ. Sci. Pollut. Res.*, 2014, **21**, 9529–9537.

33 Z. Shah, M. Gulzar, F. Hasan and A. A. Shah, *Polym. Degrad. Stab.*, 2016, **134**, 349–356.

34 A. Magnin, E. Pollet, R. Perrin, C. Ullmann, C. Persillon, V. Phalip and L. Avérous, *Waste Manag.*, 2019, **85**, 141–150.

35 J. Schmidt, R. Wei, T. Oeser, L. A. Dedavid e Silva, D. Breite, A. Schulze and W. Zimmermann, *Polymers*, 2017, **9**, 65.

36 Z. Shah, L. Krumholz, D. F. Aktas, F. Hasan, M. Khattak and A. A. Shah, *Biodegradation*, 2013, **24**, 865–877.

37 X. Jin, J. Dong, X. Guo, M. Ding, R. Bao and Y. Luo, *Polym. Int.*, 2022, **71**, 1384–1392.

38 R. Wei and W. Zimmermann, *Microbiol. Biotechnol.*, 2017, **10**, 1308–1322.

39 R. Koshti, L. Mehta and N. Samarth, *J. Polym. Environ.*, 2018, **26**, 3520–3529.

40 A. Carniel, V. de Abreu Waldow and A. M. de Castro, *Biotechnol. Adv.*, 2021, **52**, 107811.

41 W. Zimmermann, *Philos. Trans. R. Soc.*, 2020, **378**, 20190273.

42 C. M. Carr, D. J. Clarke and A. D. Dobson, *Front. Microbiol.*, 2020, **11**, 571265.

43 Y.-H. V. Soong, M. J. Sobkowicz and D. Xie, *Bioengineering*, 2022, **9**, 98.

44 S. Chen, L. Su, J. Chen and J. Wu, *Biotechnol. Adv.*, 2013, **31**, 1754–1767.

45 S. Islam, L. Apitius, F. Jakob and U. Schwaneberg, *Environ. Int.*, 2019, **123**, 428–435.

46 F. Di Bisceglie, F. Quartinello, R. Vielnascher, G. M. Guebitz and A. Pellis, *Polymers*, 2022, **14**, 411.

47 Z. Jiang, X. Chen, H. Xue, Z. Li, J. Lei, M. Yu, X. Yan, H. Cao, J. Zhou, J. Liu, M. Zheng, W. Dong, Y. Li and Z. Cui, *J. Hazard. Mater.*, 2024, **472**, 134493.

48 Z. Zhang, S. Huang, D. Cai, C. Shao, C. Zhang, J. Zhou, Z. Cui, T. He, C. Chen, B. Chen and T. Tan, *Green Chem.*, 2022, **24**, 5998–6007.

49 M. Oda, Y. Yamagami, S. Inaba, T. Oida, M. Yamamoto, S. Kitajima and F. Kawai, *Appl. Microbiol. Biotechnol.*, 2018, **102**, 10067–10077.

50 V. Tournier, C. M. Topham, A. Gilles, B. David, C. Folgoas, E. Moya-Leclair, E. Kamionka, M. L. Desrousseaux, H. Texier, S. Gavalda, M. Cot, E. Guémard, M. Dalibey, J. Nomme, G. Cioci, S. Barbe, M. Chateau, I. André, S. Duquesne and A. Marty, *Nature*, 2020, **580**, 216–219.

51 L. Aristizábal-Lanza, S. V. Mankar, C. Tullberg, B. Zhang and J. A. Linares-Pastén, *Front. Chem. Eng.*, 2022, **4**, 1048744.

52 Q. Huang, M. Hiyama, T. Kabe, S. Kimura and T. Iwata, *Biomacromolecules*, 2020, **21**, 3301–3307.

53 M. Guicherd, M. Ben Khaled, M. Guérout, J. Nomme, M. Dalibey, F. Grimaud, P. Alvarez, E. Kamionka, S. Gavalda, M. Noël, M. Vuillemin, E. Amillastre, D. Labourdette, G. Cioci, V. Tournier, V. Kitpreechavanich, P. Dubois, I. André, S. Duquesne and A. Marty, *Nature*, 2024, **631**, 884–890.

54 Q. Huang, S. Kimura and T. Iwata, *Biomacromolecules*, 2023, **24**, 5836–5846.

55 E. Bioplastics, Bioplastics Market Development Update, European Bioplastics, <https://www.european-bioplastics.org/market/>, 2022, (accessed: 28th May 2025).

56 J. Liu, J. He, R. Xue, B. Xu, X. Qian, F. Xin, L. M. Blank, J. Zhou, R. Wei, W. Dong and M. Jiang, *Biotechnol. Adv.*, 2021, **48**, 107730.

57 A. M. Radzi, S. M. Sapuan, M. Jawaid and M. R. Mansor, *Fibers Polym.*, 2017, **18**, 1353–1358.

58 J. Datta and P. Kasprzyk, *Polym. Eng. Sci.*, 2018, **58**, E14–E35.

59 H. S. Kim, M. H. Noh, E. M. White, M. V. Kandefer, A. F. Wright, D. Datta, H. G. Lim, E. Smiggs, J. J. Locklin, M. A. Rahman, A. M. Feist and J. K. Pokorski, *Nat. Commun.*, 2024, **15**, 3338.

60 N. Nagasundaram, R. S. Devi, M. K. Rajkumar, K. Sakthivelrajan and R. Arravind, *Mater. Today: Proc.*, 2021, **45**, 2286–2288.

61 I. Koutsamanis, M. Spoerk, F. Arbeiter, S. Eder and E. Roblegg, *Polymers*, 2020, **12**, 2950.

62 J. M. Stormonth-Darling, A. Saeed, P. M. Reynolds and N. Gadegaard, *Macromol. Mater. Eng.*, 2016, **301**, 964–971.

63 B. Finnigan, D. Martin, P. Halley, R. Truss and K. Campbell, *J. Appl. Polym. Sci.*, 2005, **97**, 300–309.

64 OECD, OECD Guidelines for the Testing of Chemicals, Report 9264140182, OECD Publishing, 1992.

65 F. W. Studier, *Protein Expression Purif.*, 2005, **41**, 207–234.

66 Q. Huang, S. Kimura and T. Iwata, *Polym. Degrad. Stab.*, 2021, **190**, 109647.

67 J. P. Santerre and R. S. Labow, *J. Biomed. Mater. Res.*, 1997, **36**, 223–232.

68 R. Wei, D. Breite, C. Song, D. Gräsing, T. Ploss, P. Hille, R. Schwerdtfeger, J. Matysik, A. Schulze and W. Zimmermann, *Adv. Sci.*, 2019, **6**, 1900491.

69 M. Ganesh, R. N. Dave, W. L'Amoreaux and R. A. Gross, *Macromolecules*, 2009, **42**, 6836–6839.

70 OECD, SIDS Initial Assessment Report for Adipic Acid (CAS No. 124-04-9), UNEP Publications, 2004.

71 European Chemicals Agency, 2010, <https://echa.europa.eu/de/home>, (accessed: 28th August 2025).

72 J. Drzeżdżon and J. Datta, *Waste Manage.*, 2025, **198**, 21–45.

73 K. Skleničková, S. Abbrent, M. Halecký, V. Kočí and H. Beneš, *Crit. Rev. Environ. Sci. Technol.*, 2022, **52**, 157–202.

74 M. J. C. Espinosa, A. C. Blanco, T. Schmidgall, A. K. Atanasoff-Kardjalieff, U. Kappelmeyer, D. Tischler, D. H. Pieper, H. J. Heipieper and C. Eberlein, *Front. Microbiol.*, 2020, **11**, 404.

75 J. Liu, Q. Zeng, H. Lei, K. Xin, A. Xu, R. Wei, D. Li, J. Zhou, W. Dong and M. Jiang, *J. Hazard. Mater.*, 2023, **448**, 130776.

